THE JOURNAL OF PHYSICAL CHEMISTRY A LETTERS

2007, *111,* 1167−1171
Published on Web 01/31/2007

Potential Role of the Nitroacidium Ion on HONO Emissions from the Snowpack

Stig Hellebust, Tristan Roddis, and John R. Sodeau*

Department of Chemistry, University College Cork, Ireland

Received: December 1, 2006; In Final Form: January 12, 2007

The effects of photolysis on frozen, thin films of water-ice containing nitrogen dioxide (as its dimer dinitrogen tetroxide) have been investigated using a combination of Fourier transform reflection−absorption infrared (FT-RAIR) spectroscopy and mass spectrometry. The release of HONO is ascribed to a mechanism in which nitrosonium nitrate ($NO^+NO_3^-$) is formed. Subsequent solvation of the cation leads to the nitroacidium ion, H_2ONO^+, i.e., protonated nitrous acid. The pathway proposed explains why the field measurement of HONO at different polar sites is often contradictory.

Introduction

The polar snowpack can have a major influence on the overlying atmosphere. It does not appear to inhibit emissions from land and ocean surfaces, as might be thought simplistically; rather there is increasing evidence that it can act as a source. Indeed, for some years it has been recognized that impurities present in Arctic snow can be photolyzed to release reactive trace gases into the boundary layer. As outlined below, the chemical mechanisms by which these processes are driven have been investigated in the laboratory using a number of techniques to explain unusual field observations. In this regard, one of the most intriguing recent findings has been the periodic detection of NO_x and HONO emissions from certain sunlit snowpacks located at the poles. The phenomenon was first encountered during summertime at Summit in Greenland during the PSE98 campaign by Honrath et al.[1] The findings were subsequently confirmed by a number of other measurement campaigns. For example, noon-time HONO fluxes of 5−10 nmol m^{-2} h^{-1} were found at Summit[2] during 2000 and ca. 40 nmol m^{-2} h^{-1} fluxes were later determined at Alert[3] in the Canadian High Arctic during 2000. Beyond the necessity for sunlight to initiate the releases, the presence of acidified snow also appeared, in the earliest studies, to be a common factor. Thus the absence of measurable HONO fluxes in the marine Arctic at Ny-Ålesund was attributed to the presence of local alkaline snow surfaces.[4] However, recent data obtained at a Southern Hemisphere site in Browning Pass, Antarctica,[5] indicate that fluxes of nitrous acid were measured to be close to zero even though both acidic snow and abundant UV light were present. Clearly, much more polar field data are required to establish the full conditions for HONO release.

In the meantime, a number of laboratory-based experiments have been undertaken by various research groups to clarify the potential chemical mechanisms, which may operate in the field. Both water-ices and artificial snows have been investigated and, from the results obtained, a photolysis-driven process involving acidified nitrate and nitrite ions appears to operate.[6−10] The chemistry is summarized in reactions 1−3.

$$NO_3^- + h\nu \rightarrow NO_2 + O^- \quad (1)$$

$$NO_3^- + h\nu \rightarrow NO_2^- + O \quad (2)$$

$$NO_2^- + H_3O^+ \leftrightarrow HONO + H_2O \quad (3)$$

The proposed reaction sequence is analogous to that often suggested to proceed in solution.[11] However, the efficiency of reaction 2 is extremely low with a measured quantum yield (Φ) of about 0.001. In contrast, reported Φ_1 values for NO_2 production are some 10−100 times greater than the nitrite-forming route.[12] In these experiments, initial excitations into both the stronger $\pi\pi^*$ state and the lower energy, weaker $n\pi^*$ state of the nitrate ion have been investigated. Although the latter is directly populated on the snowpack by solar radiation, it would also be rapidly formed after absorption into the $\pi\pi^*$ state via the process of internal conversion. In fact, the product observations are in line with the general expectation that $n\pi^*$ photochemistry leads to bond breaking whereas $\pi\pi^*$ photochemistry leads to isomerization. In summary, the direct production of HONO via reaction 3 might be expected to be negligible at the poles if the photolysis of nitrate ions was indeed the driving force, especially with the solar fluxes and absorbance values involved.

However, the fact remains that HONO is formed at the poles and its subsequent photochemistry can lead, in principle, to the formation of OH radicals, above snowpacks in sunlit conditions.[3] These would be produced either by direct photolysis of the HONO product in (3) or from O^- ion reaction with any hydroxonium ions present.

$$H_3O^+ + O^- \rightarrow H_2O + OH \quad (4)$$

Another route for the production of OH radicals is the photolysis of hydrogen peroxide present in snow. In fact, it has been shown that the pathway is some 10−100 times more efficient than the corresponding nitrate photolysis route for OH radical production.[13] Actual field emissions will therefore depend on relative concentrations of the two potential sources.

10.1021/jp068264g CCC: $37.00

The photolysis of artificial snow created from *basic* nitrate ion solutions has been reported to lead to greatly enhanced NO to NO_2 yields compared to more acidic counterparts where the ratio is reversed. This finding is suggested to originate from the interplay between nitrate ions and their nitrite ion photoproducts.[6] The latter species absorb sunlight to a much greater extent than the parent in the solar output region between 315 and 350 nm.[9] Reactions 1 and 2 would therefore become superseded by reaction 5 in alkaline environments.

$$NO_2^- + h\nu \rightarrow NO + O^- \quad (5)$$

It has also been proposed that the production of the peroxynitrite ion, $OONO^-$, formed as a result of "cage-recombination" on reaction 1 might also occur. This ion is stabilized in alkaline conditions and can be photolyzed to give NO.[6] The sequence is shown as reactions 6 and 7.

$$\{NO_2 + O^-\} \rightarrow OONO^- \quad (6)$$

$$OONO^- + h\nu \rightarrow NO + O_2^- \quad (7)$$

In fact, there is good experimental evidence for the formation of $OONO^-$ ions upon photolysis of nitrate ions in aqueous solution albeit at wavelengths much lower than those encountered in the snowpack and also on a very rapid time scale when the $\pi\pi^*$ state is being directly probed. Hence, femtosecond transient absorption spectroscopy has shown that the formation of $OONO^-$, in its cis-isomer, represents 44% of the *primary* photoproduct when irradiation at 200 nm is performed. Subsequent relaxation back to the nitrate ion is measured to be efficient but some of the isomer dissociates into NO and the superoxide ion.[14]

$$NO_3^- + h\nu \rightarrow ONOO^- \quad (8)$$

$$ONOO^- \rightarrow NO + O_2^- \quad (9)$$

The Φ of photoreaction 8 has been measured in aqueous solution as 0.1, a value equivalent to that measured for the production of nitrogen dioxide in reaction 1.[12] Furthermore, in one of few published studies on the photolysis of nitrate ions on water-ice, it has been shown, by use of FT−IR spectroscopy, that ammonium nitrate photodecomposes to $OONO^-$ ions. In contrast, the photolysis of frozen nitric acid hydrates was shown to lead only to the formation of molecular nitric acid in a proton-transfer mechanism.[15]

The effect of pH on the photochemistry of the system is certainly complex because the simple equilibrium step shown in reaction 3 does not describe the system over the full range of pH encountered on polar frozen surfaces. Hence, aqueous solutions of nitrite ions are not observed, by UV−vis spectroscopy, to be free of nitrous acid contributions until a pH of ca. 10 is reached; between pH 3 and 10, varying mixtures of the strongly UV-absorbing species HONO along with NO_2^- ions are present; and at pHs below 3, protonated HONO, i.e., the nitroacidium ion, H_2ONO^+, appears.[16]

Undoubtedly, the photolysis of nitrate ions in/on snowpack is involved in the observed field measurements but, given the varying field observations and the reactive nature of the nitrogen dioxide product, its potential involvement in the HONO release mechanism from frozen surfaces would also appear to be worth further experimental investigation. Hence, we describe below a reflection−absorption infrared/temperature programmed desorption (RAIRS-TPD) study of NO_2 on water-ice.

Experimental Section

The experimental setup has been described in detail elsewhere,[17] and a brief description is given here only. The measurements were made using an ultrahigh vacuum chamber (UHV) fitted with vacuum compatible KBr windows in the optical path. The vacuum was maintained by an Edwards EO4 cryo-cooled oil diffusion pump, backed by a rotary vane pump: the resultant base pressure was 10^{-8} mbar or better. A gold-foil substrate was placed in thermal contact with a liquid nitrogen reservoir through tungsten rods and suspended inside the vacuum chamber. The foil was heated resistively and cleaned by heating to 500 K between experiments. For RAIRs measurements of the surface species, a Bruker Vertex 70 FTIR instrument was used with a liquid nitrogen cooled HgCdTe detector. IR spectra were collected at 4 cm^{-1} resolution and 64 scans averaged. The UHV chamber was also fitted with a quadrupole mass spectrometer (EPIC 300, Hiden Analytical UK) for gas-phase analysis of chemical release from the frozen substrates, using electron impact ionization with 70 eV ionization potential.

Nitrogen dioxide, 99.5% pure, was obtained from Merck Ltd. and used as received. The water used was of Millipore quality and degassed by repeated freeze−pump−thaw cycles.

The gases and vapors were admitted to the chamber through glass dosing lines using manual or piezoelectric pulse valves and directed onto the gold substrate held at low temperatures. Dosages were measured in langmuir (1 langmuir = 10^{-6} Torr s = 1.33 mbar s). For "mixed ices" a co-deposition process utilizing two or more compounds was developed. It entailed simultaneous exposure of appropriate vapors from separate vessels containing the chemicals to the substrate. Mixing ratios were determined by pre-setting the piezoelectric pulse valve pulse widths for each reactant at room temperature. The pulse valves were then activated simultaneously with the desired total dosing pressure being controlled by the frequency of pulsing. Typical deposition conditions involved dosing at 70−250 langmuirs. The temperature of the substrate was continually monitored and was varied between 100 and 500 K during experiments.

For the photolysis experiments, a xenon arc lamp from ORIEL (model 60010) was employed as a broad light source solar mimic. The sample was irradiated through a quartz window on the chamber.

Results and Discussion

NO_2 on Gold. The IR spectra of *pure* NO_2 samples condensed onto the cold gold substrate, before and after photolysis, are shown in Figure 1. Sharp features at 1300 and 785 cm^{-1} accompanied by a weaker doublet at 1760/1731 cm^{-1} are readily observable in Figure 1a following deposition of NO_2 at 115 K. These bands are, in fact, due to the D_{2h} symmetric dimer of nitrogen dioxide, N_2O_4. They have been previously assigned by several researchers as the $\nu_s(NO_2)$, $\delta(NO_2)$, and $\nu_{as}(NO_2)$, modes respectively.[18−20] Indeed, the RAIRS relative band intensity measurements are consistent with the D_{2h}-N_2O_4 molecules being adsorbed to the surface with their central N−N axis aligned perpendicular to the surface.[21] The dimerization occurs readily because the equilibrium process, $2NO_2 \leftrightarrow N_2O_4$, is highly temperature-dependent and, at the concentrations employed in these experiments, is pushed efficiently to full

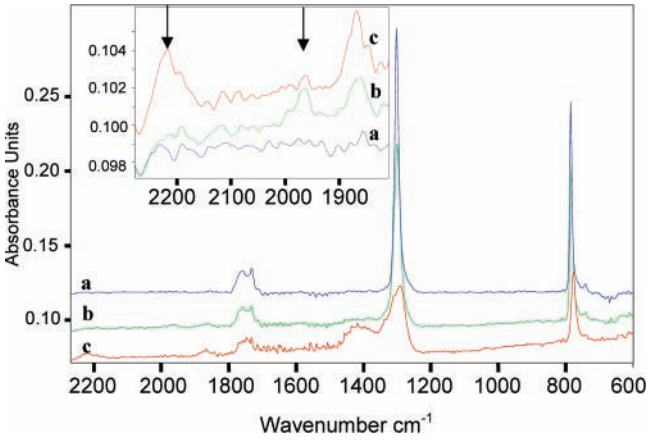

Figure 1. Spectra of NO_2 deposited on gold at 115 K (a) and following 20 min UV irradiation (b) and 70 min UV irradiation (c). The inset shows expanded view of the region 2300−1800 cm^{-1}. Arrows in the inset indicate bands at 2217 and 1961 cm^{-1}, discussed in text.

association.[22] Indeed, no spectral evidence for the presence of NO_2 molecules on the surface was obtained.

After photolysis of the low-temperature films described above, three main sets of IR bands were recorded (Figure 1b). The first consists of two peaks observed at 1961 and 2217 cm^{-1}. Their relative absorbances depend upon exposure time with the latter band clearly growing at the expense of the other. Such behavior indicates that secondary photochemistry is occurring, and indeed, after prolonged photolysis time, only the higher wavenumber peak of the two is seen to remain (Figure 1c). This photochemistry is readily explainable in terms of the initial production of the D'-N_2O_4, dinitrogen tetroxide dimer, $ONONO_2$. This species is subsequently photolyzed to produce the nitrosonium ion, NO^+. The solid-phase infrared spectra have been reported previously for both these species with the band at 1961 cm^{-1} corresponding almost exactly to that determined for the D'-isomer trapped in a low-temperature argon matrix.[20,23−26]

A second group of IR bands are measured at 1420, 1337, 1035, and 823 cm^{-1}; these can all be assigned to nitrate ions. Finally, a third set of bands, much weaker in intensity than the above features, are observed at 1864 and 1590 cm^{-1}. They represent, respectively, clear diagnostics of the formation of NO[17] and subsequently the asymmetric form of N_2O_3.[27] Both species are expected to be formed at low concentrations in the chemical system investigated here from homolytic photolysis of any of the nitrogen oxides present.

The above results indicate that photolysis of nitrogen dioxide deposited on a low-temperature gold surface proceeds as follows:

$$D_{2h}\text{-}N_2O_4\ (\text{ads}) + h\nu \rightarrow ONONO_2 \qquad (10)$$

$$ONONO_2 + h\nu \rightarrow NO^+ + NO_3^- \qquad (11)$$

Annealing the surface to 210 K causes the IR spectrum of the photolyzed thin film to change abruptly to one consisting of a single strong band at 1386 cm^{-1} accompanied by two weaker features at 2229 and 1035 cm^{-1}. At 220 K the smaller features are lost, leaving only one strong band remaining at 1374 cm^{-1}. These shifts originate with a change in phase, from amorphous to crystalline, for the nitrosonium nitrate species formed in reaction 11. The transition has been discussed in detail previously by Givan and Loewenschuss.[24]

Thermal analogues to the photoprocesses discussed above, which lead to the formation of the nitrosonium ion, have been

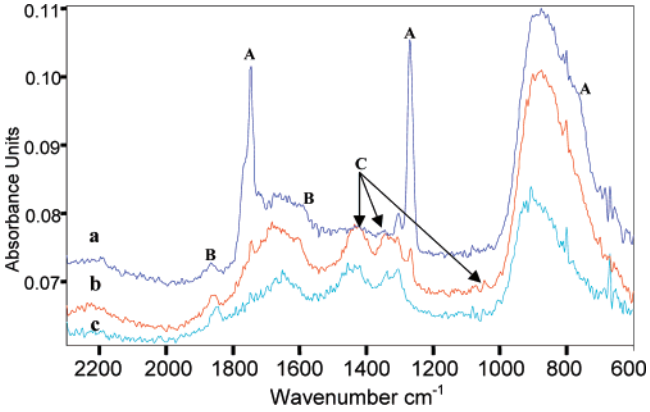

Figure 2. RAIRS spectra of, from the top down: NO_2/H_2O co-deposited at 110 K (a); same film after 60 min UV photolysis (b); same film annealed and held at 190 K (c). Capital letters refer to band groupings as discussed in text.

observed previously for nitrogen dioxide dimers. For example, reactive zeolite surfaces apparently promote the reaction by autoionisation[28] as do polluted water films.[29]

NO_2 on Water-Ice. Co-deposition of NO_2 and water vapor onto the gold foil substrate held at 110 K resulted in the IR spectrum shown in Figure 2. Hence, before photolysis a strong grouping of bands with similar absorbance values appear at 1765/1745, 1269, and 765 cm^{-1} (group A in Figure 2), although the latter feature is somewhat obscured by the broad water librational mode. Such a RAIRS spectrum indicates that the D_{2h}-N_2O_4 molecules are not ordered on the cold surface; rather, they should be considered as an amorphous dispersion within the water-ice matrix. Much weaker features at 1866 and 1595 cm^{-1} (group B in Figure 2) are again observed and represent the presence of very small amounts of NO and N_2O_3. Weak bands at 1303 and 1422 cm^{-1} are also apparent and due to the formation of the nitrate ion.

One hour photolysis of the ice film results in almost the complete loss of the strong grouping of IR bands. In addition, new bands appear at 1430, 1341, and 1044 cm^{-1} (group C in Figure 2). Very weak bands at 3525, 3225, and 2748 cm^{-1} are also measurable in absorbance difference spectra. A rather weak band at 2230 cm^{-1} is also apparent and is both blue-shifted and broader than the feature at 2217 cm^{-1} assigned to NO^+ in the water-free experiments. Such a spectral change is a good indication of the bare ion becoming solvated or linked to another species. Indeed, the blue-shift behavior has a clear analogy with the isoelectronic CO and $CO-H_2O$ systems.[30] Here matrix isolated CO displays its IR fundamental at 2138 cm^{-1}, whereas its water-partnered counterpart absorbs at 2149 cm^{-1}.

Upon annealing to temperatures between 150 and 210 K a number of important spectral changes are observed. The largest changes are observed at temperatures above 180 K when many of the IR bands begin to be lost. Of particular note is the fact that near 205 K the 2230 cm^{-1} feature is lost entirely. These observations clearly indicate that some chemicals are emitted from the surface and possibly transformed by the warming process

To clarify the nature of the emissions, the mass spectrometer was employed to monitor the gas phase in parallel to the collection of the RAIRS data. A solid water-ice surface was first deposited and warmed to 210 K. This control experiment led to the detection of only one signal at $m/z = 18$, which is, of course, due to H_2O. Photolyzed N_2O_4 ice films were then

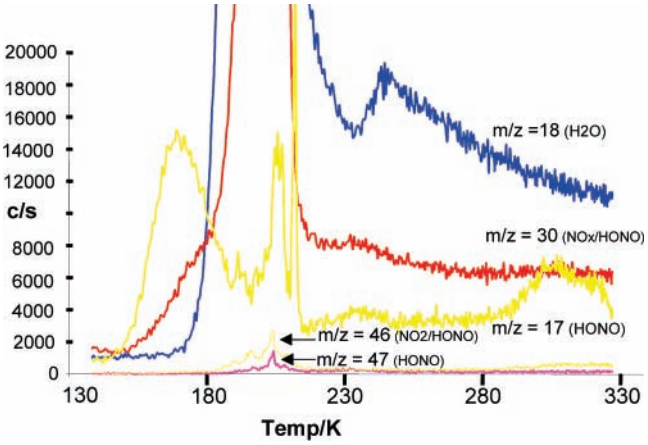

Figure 3. Thermal desorption profiles of NO_y and H_2O subsequent to photolysis of D_{2h}-N_2O_4 in water ice. The mass spectral signal $m/z = 17$ has been corrected for the contribution from water using the water fragmentation pattern 74% $m/z = 18$, 17% $m/z = 17$. The peak positions of $m/z = 17$ are 170, 200, and 210 K. The peak position of $m/z = 47$ is seen at 205 K. The peak positions of the water signal ($m/z = 18$) are 190 (shoulder), 200, and 210 K, and the peak position of $m/z = 30$ is 205 K with a minor peak at 197 K.

warmed and led to detectable gas-phase fragments with $m/z = 17$, 30, 46, and 47. These being in addition to the signature signal of water detected at $m/z = 18$. In parallel with the IR measurements, the largest increase in signal begins at about 180 K. The most likely identities for the fragments in the system studied here are OH^+ ($m/z = 17$), NO^+ ($m/z = 30$), NO_2^+ ($m/z = 46$) and $HONO^+$ ($m/z = 47$).

To investigate the processing in more detail, a temperature programmed desorption (TPD) experiment was then carried out between 150 and 340 K, employing a constant heating rate of approximately 0.8 K/s. The results indicate that the gas-phase signal for the $m/z = 17$ and 30 fragments increase gradually from 150 K, with the former maximizing at about 170 K. They increase further when the $m/z = 18$ (water signal) starts increasing around 170 K. At about 205 K the signals for the fragments $m/z = 17$, 30, 46, and 47 reach a maximum: this being the same temperature at which the IR band for the NO^+ species is lost. The experimental behavior is summarized in Figure 3. As an additional note, desorption of a sample film consisting purely of a mixture of NO and NO_2 gives two peaks in the $m/z = 30$ signal, at approximately 130 and 160 K.

An alternative method of producing the cold thin films was also employed. Here nitrosonium nitrate was formed initially by photolysis of a D_{2h}-N_2O_4 film and a layer of water-ice was deposited on top. To promote mixing, the solid was then annealed to temperatures between 190 and 200 K. RAIRS spectra were taken at all stages, and the most noteworthy infrared features observed in addition to bands, which can be assigned to the nitrate ion, were two strong bands at 3430 and 1130 cm^{-1}. These features are similar to those monitored after annealing a nitric acid/water film to 200 K, as shown in Figure 4.

From previous RAIRS studies, the absorptions at 3430 cm^{-1} and 1130 cm^{-1} can be taken as evidence for the formation of nitric acid trihydrate (NAT). The bands can be assigned to the $\nu_{1,3}(H_2O)$ and $\nu_2(H_3O^+)$, oxonium ion modes of NAT, respectively.[15] They persist at temperatures higher than that at which the NO^+ species is lost, i.e., above ~205 K. The continued presence of the main nitrate ion feature around 1425 cm^{-1}, despite the loss of NO^+ implies that the oxonium ion then takes over the role of counterion.

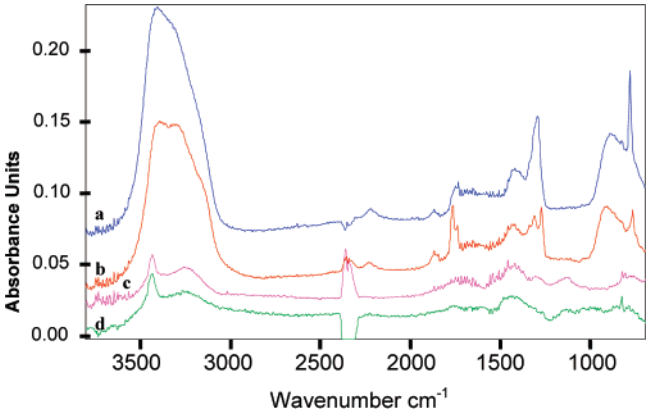

Figure 4. RAIRS spectra of, from the top down: NO_2 deposited at 110 K and photolyzed for 70 min with a top layer of water ice added subsequently (a); same film annealed and held at 190 K (b) and 200 K (c). Nitric acid deposited at 115 K and annealed to 200 K (d) is shown for comparison.

Taken together, the IR and mass spectrometry results indicate that the following mechanism operates in a water-ice thin film:

$$NO^+ + H_2O \rightarrow \{(H_2O)NO\}^+ \quad (12)$$

$$\{(H_2O)NO\}^+ + H_2O \rightarrow HONO + H_3O^+ \quad (13)$$

$$H_3O^+ + NO_3^- \rightarrow \{H_3O^+NO_3^-\} \quad (14)$$

In the overall process, NO^+ produced on the ice surface by photolysis of the nitrogen dioxide dimer becomes solvated with water and is then hydrolyzed to HONO, which is efficiently released to the gas phase. In contrast, the nitrate component is retained on the surface as NAT. The chemistry is presumably in addition to the simple photodesorption event, producing NO_2 in the gas phase, observed by Rieley et al. when wavelengths with $\lambda > 360$ nm were used.[31]

As a caveat, the minor release of HONO observed between 150 and 170 K in the TPD experiments can be explained by hydrolysis of the small amount of the asymmetric form of N_2O_3 present in the experiments, as previously discussed by Finlayson-Pitts.[29]

$$ONNO_2 + H_2O \rightarrow HONO + HONO \quad (15)$$

The important question arises: does the photochemistry discussed above have a relevance to the snowpack observations? On ice surfaces, the monomer NO_2 has an adsorption enthalpy of −22 kJ/mol,[32] whereas the dimer N_2O_4 has an adsorption enthalpy of around −40 kJ/mol[33] However, it remains a question of debate whether typical ppb concentrations of NO_2 from airborne sources of pollution could be transformed to the dimer efficiently on cold, polar surfaces. Thus from the equilibrium data the *fraction* of N_2O_4 formed in the gas phase in the ppb NO_2 range would be $\sim 10^{-7}$ at 270 K and $\sim 10^{-4}$ at 210 K. Neglecting differences in entropic contributions to the adsorption equilibrium constant between NO_2 and N_2O_4, one can subsequently calculate that the *fraction* of N_2O_4 on a surface would only range from 10^{-3} at 270 K to 0.4 at 210 K.[32] On the other hand, computer modeling calculations have shown that nitrogen dioxide dimer species are significantly more strongly bound to surfaces containing −OH groups than monomer counterparts.[34]

The fact remains that when sufficient concentrations of nitrogen dioxide are present in snowpack regions, the surface

chemistry described in the current experiments could operate to act as the HONO and NO release mechanism. Such a pathway may well be important as the quantum yield of reaction 2 is so low.[12] Furthermore, the UV−visible absorption cross sections for low-temperature N_2O_4 have been measured to be considerably higher than nitrate ions in the important solar region around 350 nm.[35] A photolysis mechanism would then appear to be possible from the above results, although a hydrolytic disproportionation of NO_2 into nitrite and nitrate ions might also occur, as previously discussed.[10]

One potential source of significant quantities of frozen nitrogen dioxide originates from the photolysis of nitrate ions (via reaction 1) concentrated within ice "micropockets". Depending upon acidity, the subsequent photoproduction of the nitroacidium ion may lead to release of HONO, especially if no other reactants are present. However, if organic compounds are present, the solvated NO^+ may, in preference, act as a nitrosating agent,[36] leading to little or no HONO release. Such constrained micro-environments have been proposed to drive other polar-related chemistry, e.g., the release of interhalogens to the troposphere, although it remains to be seen whether they exist in actual snowpacks.[37]

Acknowledgment. We acknowledge financial support from INTAS, the EU Marie Curie programme, and the Norwegian Research Council. Inputs from Dr. M. Ammann and Dr. A Grammas are also gratefully acknowledged.

References and Notes

(1) Honrath, R. E.; Peterson, M. C.; Dziobak, M.; Dibb, J.; Arsenault, M.; Green, S. *Geophys. Res. Lett.* **2000**, *27*, 2237.
(2) Honrath, R.; Lu, Y.; Peterson, M.; Dibb, J.; Arsenault, M. *Atmos. Environ.* **2002**, *36*, 2629.
(3) Zhou, X.; Beine, H. J.; Honrath, R. E.; Fuentes, J. D.; Simpson, W.; Shepson, P. B.; Bottenheim, J. W. *Geophys. Res. Lett.* **2001**, *28*, 4087.
(4) Beine, H. J.; Dominé, F.; Ianniello, A. M. N.; Allegrini, I.; Teinilä, K.; Hillamo, R. *Atmos. Chem. Phys.* **2003**, *3*, 335.
(5) Beine, H. J.; Amoroso, A.; Dominé, F.; King, M. D.; Nardino, M.; Ianniello, A.; France, J. L. *Atmos. Chem. Phys. Discuss.* **2006**, *6*, 615.
(6) Honrath, R. E.; Guo, S.; Peterson, M.; Dziobak, M.; Dibb, J.; Arsenault, M. *J. Geophys. Res.-Atmos.* **2000**, *105*, 24183.
(7) Domine, F.; Shepson, P. B. *Science* **2002**, *297*, 1506.
(8) Boxe, C. S.; Colussi, A. J.; Hoffmann, M.; Murphy, J.; Wooldridge, P.; Bertram, T.; Cohen, R. *J. Phys. Chem. A* **2005**, *109*, 8520.
(9) Jacobi, H.; Annor, T.; Quansah, E. *J. Photochem. Photobiol. A-Chem.* **2006**, *179*, 330.
(10) Boxe, C. S.; Colussi, A. J.; Hoffmann, M.; Perez, I.; Murphy, J.; Cohen, R. *J. Phys. Chem. A* **2006**, *110*, 3578.
(11) Mack, J.; Bolton, J. *J. Photochem. Photobiol. A-Chem.* **1999**, *128*, 1.
(12) Mark, G.; Korth, H.-G.; Schuchmann, H.-P.; von Sonntag, C. *J. Photochem. Photobiol. A-Chem.* **1996**, *101*, 89.
(13) Chu, L.; Anastasio, C. *J. Phys. Chem. A* **2005**, *109*, 6264.
(14) Madsen, D.; Larsen, J.; Jensen, S.; Keiding, S.; Thøgersen, J. *J. Am. Chem. Soc.* **2003**, *125*, 15571.
(15) Koch, T. G.; Holmes, N. S.; Roddis, T. B.; Sodeau, J. R. *J. Phys. Chem.* **1996**, *100*, 11402.
(16) Riordan, E.; Minogue, N.; Healy, D.; O'Driscoll, P.; Sodeau, J. *J. Phys. Chem. A* **2005**, *109*, 779.
(17) Horn, A. B.; Koch, T. G.; Chesters, M.; McCoustra, M.; Sodeau, J. *J. Phys. Chem.* **1994**, *98*, 946.
(18) Wang, J.; Koel, B. E. *Surf. Sci.* **1999**, *436*, 15.
(19) Wang, J.; Koel, B. E. *J. Phys. Chem. A* **1998**, *102*, 8573.
(20) Jones, L. H.; Swanson, B. I.; Agnew, S. F. *J. Chem. Phys.* **1985**, *82*, 4389.
(21) Koch, T. G.; Horn, A. B.; Chesters, M.; McCoustra, M.; Sodeau, J. *J. Phys. Chem.* **1995**, *99*, 8362.
(22) Atkinson, R. *J. Phys. Chem. Ref. Data* **1997**, *26*, 690.
(23) Hisatsune, I. C.; Devlin, J. P.; Wada, Y. *J. Chem. Phys.* **1960**, *33*, 714.
(24) Givan, A.; Loewenschuss, A. *J. Chem. Phys.* **1990**, *93*, 7592.
(25) Givan, A.; Loewenschuss, A. *J. Chem. Phys.* **1989**, *90*, 6135.
(26) Breuer, H.; Kuger, J. *Ber. Busen-Ges. Phys Chem.* **1978**, *82*, 97.
(27) Melen, F.; Pokorni, F.; Herman, M. *Chem. Phys. Lett.* **1992**, *194*, 181.
(28) Yeom, Y. H.; Wen, B.; Sachtler, W. M. H.; Weitz, E. *J. Phys. Chem. B* **2004**, *108*, 5386.
(29) Finlayson-Pitts, B. J.; Wingen, L. M.; Sumner, A. L.; Syomin, D.; Ramazan, K. A. *Phys. Chem. Chem. Phys.* **2003**, *5*, 223.
(30) Abe, H.; Yamada, K. M. T. *J. Chem. Phys.* **2001**, *114*, 6134.
(31) Rieley, H.; McMurray, D.; Haq, S. *J. Chem. Soci., Faraday Trans.* **1996**, *92*, 933.
(32) Bartels-Rausch, T.; Eichler, B.; Zimmermann, P.; Gäggeler, H. W.; Ammann, M. *Atmos. Chem. Phys.* **2002**, *2*, 235.
(33) Rieley, H.; Colby, D. J.; McMurray, D.; Reeman, S. M. *Surf. Sci.* **1997**, *390*, 243.
(34) Thompson, K. C.; Margey, P. *Phys. Chem. Chem. Phys.* **2003**, *5*, 2970−2975.
(35) Harwood, M.; Jones, R. *J. Geophys. Res.* **1994**, *99*, 22955.
(36) Grossi, L.; Montevecchi, P. *J. Org. Chem.* **2002**, *67*, 8625.
(37) O'Driscoll, P.; Lang, K.; Minogue, N.; Sodeau, J. *J. Phys. Chem. A* **2006**, *110*, 4615.